THE PUBLISHING HOUSE
OF THE ROMANIAN ACADEMY

PROCEEDINGS OF THE ROMANIAN ACADEMY, Series A,
Volume 16, Number 2/2015, pp. 217–225

APPLICATION OF RESPONSE SURFACE METHODOLOGY FOR STUDY OF EFFECTIVE STRAIN IN EQUAL CHANNEL ANGULAR PRESSING OF AA6061 ALLOY

Reza NEMATI-CHARI[1], Kamran DEHGHANI[2], Abdolvahed KAMI[1], Dorel BANABIC[3]

[1] Amirkabir University of Technology, Mechanical Engineering Department, Iran
[2] Amirkabir University of Technology, Mining & Metallurgy Engineering Department, Iran
[3] CERTETA Research Centre, Technical University of Cluj-Napoca, Romania
E-mail: banabic@tcm.utcluj.ro

In this paper, the effect of equal-channel angular pressing parameters including die channel angle (ϕ), die outer corner angle (ψ), fillet radius (r), friction coefficient between billet and punch (μ) and friction factor between billet and die (m) on the equivalent plastic strain of AA6061 alloy is investigated. In this regard, the equal-channel angular pressing is modeled by the commercial finite element software, ABAQUS/Explicit. Then the response surface methodology is used for design of experiments and development of a simple and efficient model for prediction of the equivalent plastic strain in equal-channel angular pressing with respect to the process parameters. The microstructure of specimens after equal-channel angular pressing is analyzed by transmission electron microscopy. The results showed that the dislocation density and the fraction of formed grains (sub-grains) increased after equal-channel angular pressing. Furthermore, the mechanical properties of AA6061 alloy after applying two passes of equal-channel angular pressing in route-C are examined. It was found that the response surface analysis is a useful tool in modeling and optimization of the equivalent plastic strain. The results of response surface analysis showed that the die channel angle and die outer corner angle are the most significant parameters while the other parameters have no considerable effect on the equivalent plastic strain.

Key words: equal channel angular pressing, severe plastic deformation, ultra-fine grained, response surface methodology.

1. INTRODUCTION

Equal channel angular pressing (ECAP) process was originally developed by Segal [1] in the former Soviet Union to achieve bulk ultra-fine grained (UFG) metals. Compared to the traditional forming processes, the great advantage of the ECAP is that the size and shape of workpiece before and after deformation are the same. So, the workpiece can be extruded repeatedly which, result in a higher accumulated effective strain in the workpiece. Under suitable channel geometry and process variables, strain of ~1 can be imposed into the metal at a single pass through ECAP die [2, 3].

A great attention is given to create UFG microstructure via ECAP process by several researchers [4–7]. Although, it is possible to impose sever plastic strains in parts using ECAP process, but if the parameters of this process is not set properly, the efficiency of the processes will reduce. For this reason, many attempts have been made to optimize the parameters in SPD processes. For example, Lu *et al.* [8] investigated the influence of channel angle on the deformation behavior and strain homogeneity in ECAP by conducting finite element simulations with COSMOS. The experimental and numerical results showed that $\phi = 110°$ and 130° gives higher homogeneity than $\phi = 70°$ and 90°. Djavanroodi *et al*. [9] investigated the effect of die channel angle, friction and back pressure in the equal channel angular pressing using 3D finite element simulation. It was observed that the strain value and homogeneity of strain distribution increase by decreasing of the die channel angle or increasing of the friction coefficient or by imposing the back punch pressure in the outlet channel.

The traditional optimization method considers one factor at a time and keeps the level of all other variables fixed. Using this method in engineering applications with multiple effective variables is expensive

and time-consuming. Furthermore, the interaction between factors is ignored in this method. Therefore, in order to overcome these disadvantages, other methods like response surface methodology (RSM) can be used in order to evaluate the effect of several factors and responses with an acceptable number of experiments. Many successful optimizations and predictions have been performed using RSM in different fields. Some examples of RSM application in the field of metal forming are as follows: Bahloul al. [10] utilized RSM to optimize of springback predicted by experimental and numerical approach. Azaouzi *et al*. [11] optimized of tool path for single point incremental sheet forming using response surface method. Qian al. [12] investigated the effect of response surface modeling and optimization of a new impact-toughened mould material used in the shaping of sanitary ware. Makadia al. [13] optimized of machining parameters for turning operations based on RSM.

The literature survey shows that the experimental and numerical investigation of ECAP has not been carried out together. So, in this research the influence of process parameters on the magnitude and distribution of the equivalent plastic strain is investigated using numerical simulation in ABAQUS software. Furthermore, RSM and analysis of variance (ANOVA) were employed to obtain the optimum values of the ECAP parameters. These parameters contain the die channel angle (ϕ), die outer corner angle (ψ), fillet radius (r), friction coefficient between billet and ram (μ) and friction factor between billet and die (m).

2. EXPERIMENTAL PROCEDURES

Figure 1a demonstrates a schematic of ECAP process. The ECAP die has two intersecting channels (at the angle of ϕ) of identical cross-section. A well lubricated billet with the same cross-section as die channel is placed in one of the channels, and a punch then presses it into the second one. Ideally, the deformation occurs by shear at the intersecting plane. The ECAP experimental setup and the ECAP die are shown in Fig. 1b. The ECAP die has the die channel angle of 110° and the outer corner angle of 20°.

The specimens are the billets of Al6061 alloy with the thickness of 14 mm, width of 50 mm and length of 100 mm. The chemical composition of this material is presented in Table 1. To obtain a uniform microstructure and elimination of residual stresses, the as received specimens were annealed at 530°C for 4 hours. Then the annealed samples were lubricated and pressed in the ECAP die at the speed of 5 mm/s.

Table 1

Chemical composition of Al6061 alloy (wt%)

Mg	Si	Cr	Cu	Fe	Al
0.9	0.73	0.19	0.2	0.37	Balance

Four different ECAP routes are available: route-A, route-BA, route-BC and route-C. In this paper, repetitive pressings of the same sample were conducted up to two passes in route-C. In route-C, the sample is rotated by 180° between the ECAP passes. Hardness of the ECAPed specimens was determined on three surfaces of specimens using Vickers hardness test by the load of 5kg for 10 seconds. The reported hardness values are the mean value of 10 readings, and the maximum deviation from the mean value was ±4%. Also, microhardness of the ECAPed specimens was determined on the side surface of specimens using Vickers microhardness test by the load of 50 g for 10 seconds with a magnification of 400. To prepare the specimens, the side surface was carefully polished to a mirror-like finish and then hardness measurements were taken following a regular rectilinear grid pattern with spacing between each measurement of 0.5 mm. Furthermore, the mechanical properties required for definition of the material in the finite element simulations were determined by conducting tensile tests.

3. FINITE ELEMENT ANALYSIS

To evaluate the equivalent plastic strain of the specimens, series of finite element simulations were performed using ABAQUS/Explicit commercial software. In these simulations, the die and the punch were

modeled as discrete rigid. The Coulomb friction model with a constant coefficient of friction μ was used between the billet and the punch. While, the friction condition between the die and the billet was modeled using the constant shear model. The Al6061 alloy was defined using the properties listed in Table 2.

Table 2

The material data for simulations of the ECAP process

Density, ρ [kg/m^3]	Poisson's ratio, υ	Young's modulus [GPa]	Yield stress [MPa]	Strength coefficient, K [MPa]	Strain hardening exponent, n
2700	0.33	68.9	33	172	0.27

The billet was meshed using C3D8R (Continuum, 3D, 8-node, Reduced integration) element type. The total number of elements of the deforming body was equal to 160398. Fig. 2 shows the equivalent plastic strain contour for one-pass ECAPed specimen.

Comparison of the maximum load obtained from finite element simulations and experiments validates the accuracy of simulations. The values of the parameters in the finite element model were selected according to the experimental condition. The geometrical parameters, the die channel angle (ϕ = 110°), die outer corner angle (ψ = 20°) and the fillet radius (r = 2 mm) were set based on the geometries of the dies and the billet used in the experimental tests. Also, the friction coefficient between punch and the billet was selected 0.13. The amount of friction factor depends on the contact surfaces. This parameter was set as 0.14 [9]. The maximum values of the experimental and numerical measured loads are 8.9 and 10.5 tonnes, respectively. Therefore, the numerical model predicts the pressing load with an acceptable error of approximately 15%.

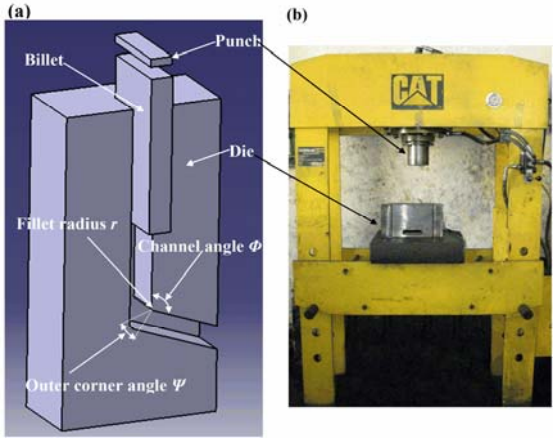

Fig. 1 – a) Schematic of the ECAP process; b) experimental set-up of ECAP process.

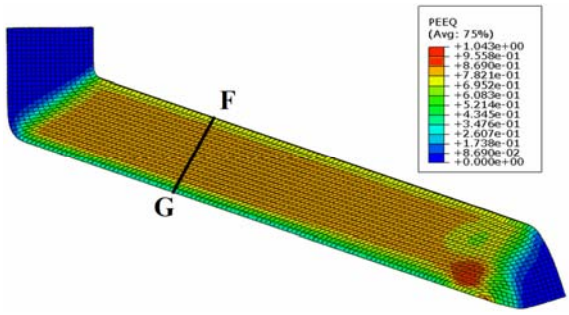

Fig. 2 – Equivalent plastic strain distribution after one-pass ECAP.

4. RESPONSE SURFACE METHODOLOGY

The most recommended types of RSM designs are Box-Behnken and Central Composite Designs (CCD). In this research, CCD was used for experimental design. The CCD itself can be classified into three types (i.e. circumscribed, inscribed and face centered). Among these CCD types, central composite inscribed (CCI) design is proper for situations in which the range of the factors is truly specified [14, 15]. In this study, since the specified upper and lower limits of the parameters (factors) have these conditions, the CCI design was used. The CCI design considers these upper and lower limits as the star points and creates a factorial or fractional factorial design within those limits.

The RSM procedure was designed based on the five-factor CCI design consisting of die channel angle (ϕ), die outer corner angle (ψ), fillet radius (r), the friction coefficient between billet and punch (μ) and the

friction factor between the billet and the die (*m*). Table 3 shows the levels of these factors and their equivalent coded values. The α value in this table is equal to 2.378 which were recommended by Design Expert 7.0 software [16]. According to this table, it is necessary to define five levels for each factor in the CCI design. A total number of 50 set of runs in RSM with different combinations of factor levels were prepared in a random order.

Table 3

Input factors and their coded and actual values used for RSM

Input parameters	Symbol	Coded levels				
		Axial (-α)	-1	0	1	Axial (+α)
Die channel angle (°)	*A*	90	107.39	120	132.61	150
Die outer corner angle (°)	*B*	0	20.28	35	49.72	70
Fillet radius (mm)	*C*	0.5	1.22	1.75	2.28	3
Friction coefficient between billet and punch	*D*	0.1	0.16	0.2	0.24	0.3
Friction factor between billet and die	*E*	0.05	0.14	0.21	0.26	0.35

5. RESULTS AND DISCUSSION

5.1. RSM RESULTS

A custom quadratic model was developed for prediction of the equivalent plastic strains. To assess the fitness of the model to the numerical data, ANOVA was employed. The ANOVA results are presented in Table 4. The *F*-value of the custom quadratic model is equal to 560.77 which implies that the model is significant. According to Table 4, there is only a 0.01% chance that this large *F*-value could occur due to noise. Prob > *F* values are usefull tools for recognition of significant terms. All terms with Prob > *F* values less than 0.05 are significant. So, according to Table 4, *A*, *B*, *AB* and A^2 are significant model terms. On the other hand, the model terms having Prob > *F* greater than 0.1 are not significant. From Table 4 one may notice that *C* (fillet radius), *D* (friction coefficient between billet and punch) and *E* (friction factor between billet and die) are not significant terms.

Another useful tool to test the statistical significance of the terms and the model, is the comparison of the sum of the squares (SS). For this purpose, the percentage ratio of SS of each term or model to total SS can be used. This ratio for the model is about 99.10% which indicates that the conducted model has high confidence level. Meanwhile, the developed model has a high *R*-square value (adjusted *R*-square is 99.56%) which, shows that the model is able to provide a good estimation of the response in the studied ranges.

Table 4

ANOVA table for equivalent plastic strain

Source	Sum of Squares	DOF	Mean Square	*F*-Value	*p*-value (Prob > *F*)
Model	1.11	20	0.056	560.77	<0.0001
A- Φ	1.1	1	1.1	11078.65	<0.0001
B- Ψ	6.76E-03	1	6.76E-03	68.03	<0.0001
C- *r*	7.74E-05	1	7.74E-05	0.78	0.3847
D- μ	2.62E-08	1	2.62E-08	2.63E-04	0.9872
E- *m*	2.57E-04	1	2.57E-04	2.59	0.1185
AB	2.06E-03	1	2.06E-03	20.77	<0.0001
A^2	3.60E-03	1	3.60E-03	36.19	<0.0001
B^2	3.28E-04	1	3.28E-04	3.3	0.0797
Residual	2.88E-03	29	9.94E-05		
Lack of Fit	2.88E-03	22	1.31E-04		
Cor Total	1.12	49			

The data provided by ANOVA was used to formulate a relationship between the response (PEEQ) and the independent input factors. The formulation was designed to only involve the significant terms. As discussed before, Prob > *F* value are utilized to find the significant terms (*A*, *B*, *AB* and A^2). Regression data analyses in Table 4 show that the fitted second-order model is highly significant. This quadratic relation for the coded levels of the factors is presented in Eq. (1). According to this equation, with increasing the die channel angle (*A*) and die outer corner angle (*B*) the PEEQ decreases. It is clear that A, regarding its bigger coefficient in the equation, is the most significant parameter affecting the PEEQ. Using Eq. (1), it is possible to calculate the coefficient of correlation (R^2) for the model. R^2 value for PEEQ is equal to 0.9974 which is quite reasonable for the response surface method. In Eq. (1) there are two second-order terms (*i.e. AB* and A^2). The P-values of these terms are less than 0.0001 which indicates that they have a significant effect on the model. But the small value of the coefficients of the second order terms of Eq. (1) imply that they don't have a significant effect on the PEEQ.

$$\text{PEEQ} = 0.66 - 0.16A - 0.012B + 0.008031AB + 0.008158A^2 . \quad (1)$$

Response surface plots are useful tools for investigation of the interaction and individual effects of the process parameters. Fig. 3a depicts the changes in PEEQ with respect to die channel angle and friction coefficient between the billet and the punch. According to this figure, regardless of the value of friction coefficient between the billet and punch, the highest value of PEEQ occurs at the lowest value of die channel angle (90°). Figure 3a shows that there is no significant change in the color and the slop of PEEQ surface plot with respect to variation of friction coefficient between the billet and punch. This indicates that the friction coefficient between the billet and punch is an insignificant factor. Figure 3b shows the interacted effects of the die outer corner angle and the friction factor between the billet and die on PEEQ. Unlike Fig. 3a, the change in the color of Fig. 3b is almost negligible in all direction. Nevertheless, it is worthwhile to investigate the combined effects of the die outer corner angle and the friction factor between the billet and die on PEEQ; since their effects on PEEQ cannot be observed when they are studied in combination with the more effective parameters like the die channel angle. From Fig. 3b one may notice that PEEQ increases with the decrease of the die outer corner angle and increase of friction factor between the billet and die. Accordingly, the highest value of PEEQ has been obtained at the lowest value of the die outer corner angle (0°) and the highest value of friction factor between the billet and die (0.35) which is about 0.68. One may notice that the slop of PEEQ surface plot along die outer corner angle axis is larger than its slop along friction factor between the billet and die axis; which implies that the die outer corner angle is more significant than the friction factor between the billet and die. Although the increase in the friction factor between the billet and die result in the increase of PEEQ but to lengthen the service time of the die, ease of billet exit from the die and reduction of process load it is recommended to use a lower friction in the process.

5.2. OPTIMIZATION

The optimum values of ECAP parameters have been obtained utilizing the data obtained by the statistical analysis. Design-Expert searches for a combination of factors that simultaneously satisfy the constraints set for each of the response and factors. These conditions are stated in Table 5. The optimum values of the factors (in their specified ranges) led to the maximum PEEQ. In this condition, the predicted PEEQ (1.17) shows an improvement about 7.34% with respect to the highest value of PEEQ (1.09) obtained by experimental design.

Table 5

Optimization goal and constraints for all factors and the response

Input parameters	Goal	Lower	Upper	Optimum
Die channel angle (°)	In range	90	150	90
Die outer corner angle (°)	In range	0	70	0
Fillet radius (mm)	In range	0.5	3	2.94
Friction coefficient between billet and punch	In range	0.1	0.3	0.12
Friction factor between billet and die	In range	0.05	0.35	0.05
Equivalent plastic strain	Maximize	0.3	1.09	1.17

5.3. EXPERIMENTAL RESULTS

Figure 4 shows the two-pass ECAPed specimens in route-C. According to this figure, the top and bottom regions of the billets experience a severe and improper deformation. These regions are the waste parts of the specimen after the ECAP process. These parts are eliminated in calculation of PEEQ.

Figure 5 depicts the TEM images of the specimens annealed at 530°C and after two passes of ECAP *via* route-C. After sever plastic deformation three types of boundaries and transformations can be seen in a grain boundary structure. These boundaries are generated at different strains, and generation of the UFG is attributed to a sequential structural cycle starting from dislocation cells evolution, polygonized dislocation walls (PDW), partially transformed boundary (PTB) and grain boundary (fine-grained structure). Many researchers have suggested mechanisms for the formation of the UFG under specific experimental conditions; however, the detailed mechanism of the transformation from a PDW into a grain boundary is not clearly explained yet. In fact, PDWs firstly transform into PTBs, and then transform into grain boundaries, the reason of this transformation process is expected to be an increase of dislocation density in these boundaries. A cell structure generated by dislocation tangle is transformed into a granular one, then when further deformation is applied the granular ones later will be transformed into the UFG by the partial annihilation of dislocations with opposite signs at the cell boundaries [17]. Valiev *et al.* [18] proposed that the transformation mechanism from PDW into a grain boundary structure can be caused by an increase of dislocation density inside these boundaries during straining.

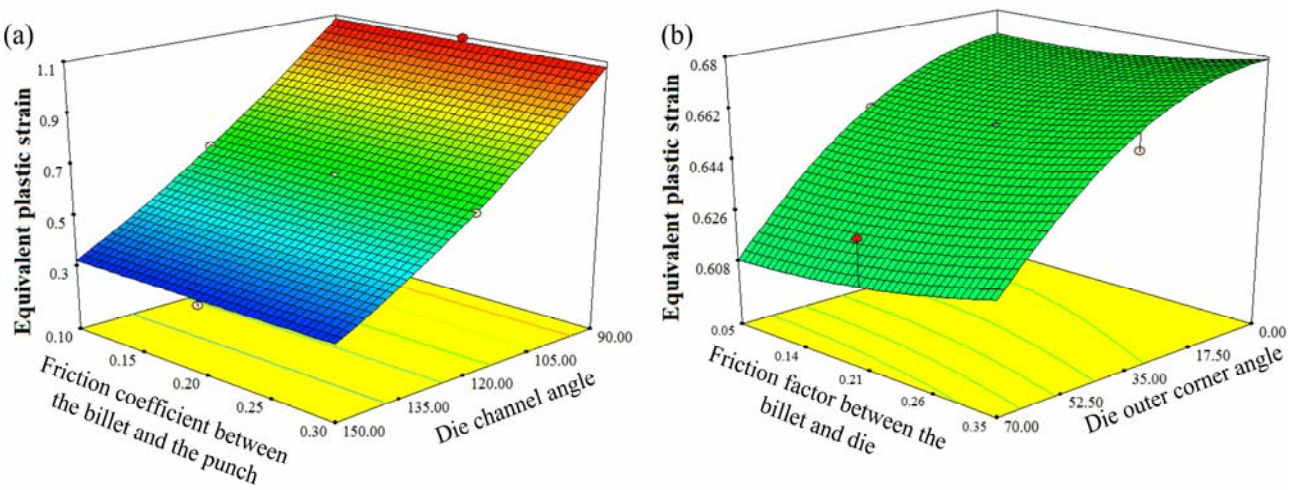

Fig. 3 – Surface plots of PEEQ with respect to: a) die channel angle and friction coefficient between the billet and the punch; b) die outer corner angle and friction factor between the billet and die.

According to Fig. 5, it can be seen that the dislocation density of the two-pass ECAPed specimen is very high and dislocations were observed to be accumulated near the grain boundaries as complex tangles and forests. From Fig. 5, one may notice that a large population of dislocations is spread both inside the grains and at the grain limits. The dislocations belong to all slipping planes and look at meted because of the important plastic strain accumulated in the structure. The average grain size cannot be established from the image due to high level of straining, the structure should consist of grain remainders, being mostly fibrous.

Figures 6 and 7 show the variation of tensile properties of the ECAPed specimens at different passes in route-C. Figure 7 shows that after the first pass, yield and ultimate strengths are increased from 33 to 94 MPa and 84 to 138 MPa, respectively, while the elongation is reduced from 22.2% to 6.4%. During the first pass, the dislocation density at inside and boundaries of the initial grains increases and cause to strain hardening. In the second pass, the yield and ultimate strengths have further increased to 106 and 149 MPa, respectively. The elongation in the second pass decreases by 3.7%.

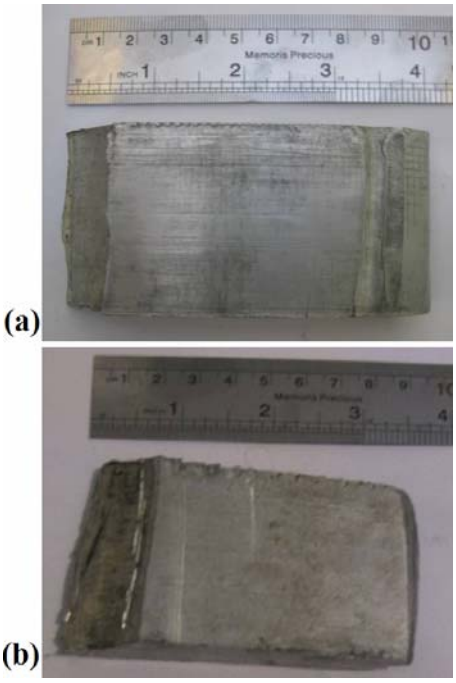

Fig. 4 – ECAPed billets *via* route-C: a) one pass ECAP; b) two passes ECAP.

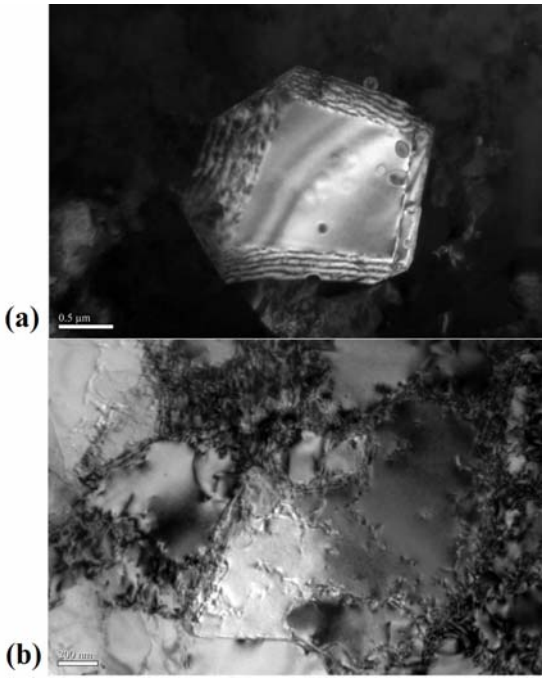

Fig. 5 – TEM images of a) the specimens annealed at 530°C; b) after two passes of ECAP via route-C.

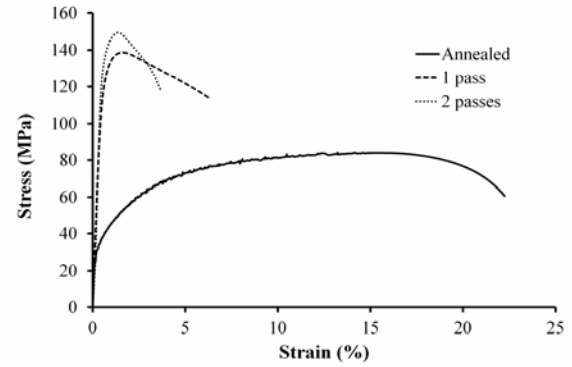

Fig. 6 – Stress-strain curves of the billets before and after ECAP in route-C.

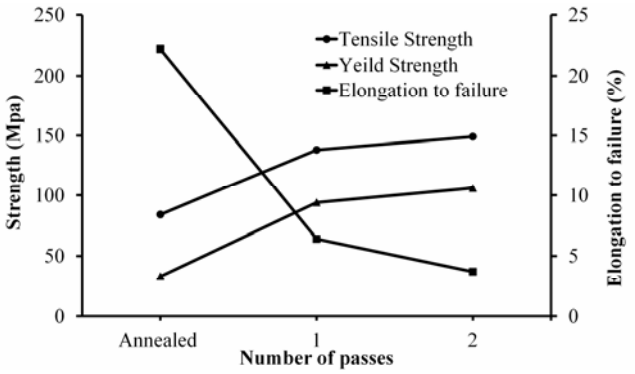

Fig. 7 – Tensile properties variations of the specimens before and after ECAP as a function of the number of passes for route-C.

Figure 8 shows the variation of hardness values of the specimens before and after ECAP as a function of the number of ECAP passes *via* route-C in three surfaces. According to this figure the hardness increases after the first pass of ECAP. The high rate of increase in hardness at the first pass can be associated to strain hardening effect due to increased dislocation density. After the first pass, the strain hardening is not the dominant mechanism in the hardening process. As a result, the rate of hardness increase is reduced at the second pass. It is clear that the hardness in the middle surface of the billet is higher than top and bottom surfaces due to use of the lubrication and also because of the concentration of larger plastic deformation in the middle surface of the billet. In the second pass of ECAP, hardness in middle surface of the billet is increased by 100%.

Figure 9 shows the micro-hardness values across the billet thickness (Fig. 2) before and after ECAP in route-C. According to this figure, micro-hardness increased after ECAP process. But, rate of the microhardness enhancement is reduced in the second pass. From Fig. 9 one may notice that the uniformity of micro-hardness is decreased after ECAP process. This phenomenon could be related to the reduction of strain uniformity after ECAP.

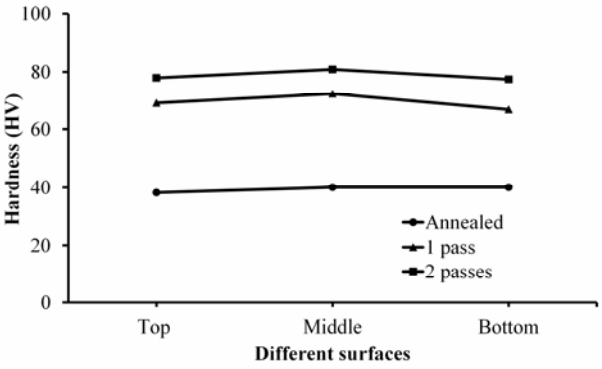

Fig. 8 – Variation of hardness of the ECAP samples with respect to the number of passes in route-C.

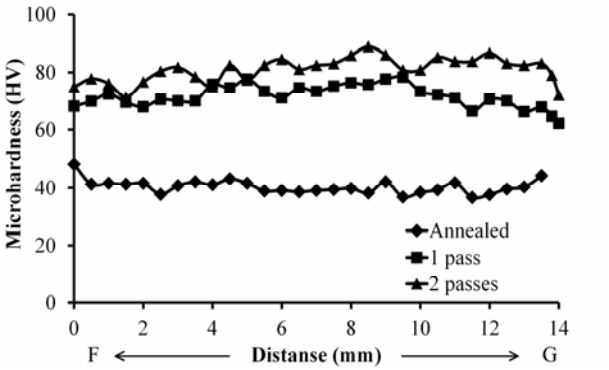

Fig. 9 – Microhardness variation of the specimens before and after ECAP in route-C across F–G section.

6. CONCLUSION

Response surface methodology, finite element analysis and experimental approaches have been used to study the Al6061 alloy billet deformation during the ECAP process with plate samples. The following results were obtained:

1 – TEM images illustrate that with the increase of accumulative strain, a large population of dislocations spread both inside the grains and at the grain boundaries.

2 – Applying severe plastic deformation by the ECAP process up to two passes in route-C causes a considerable increase in the hardness and strength and in contrast, a reduction in the elongation value. Hardness in the middle surface of the billet increase by 100% compared to the annealed state.

3 – Using response surface methodology and ANOVA, a simple and efficient quadratic model was developed to predict the PEEQ by considering the significant terms provided by ANOVA. This model can be used as a useful tool for prediction of the PEEQ with high accuracy.

4 – ANOVA showed that the die channel angle and die outer corner angle are the more significant parameters while three other parameters have no considerable effect on PEEQ (the die channel angle is the most significant parameter).

REFERENCES

1. SEGAL, V.M., *Materials processing by simple shear*, Mater. Sci. Eng. A., **197**, *2*, pp. 157-164, 1995.
2. WANG, J., IWAHASHI, Y., HORITA, Z., FURUKAWA, M., NEMOTO, M., VALIEV, R.Z., LANGDON, T.G., *An investigation of microstructural stability in an Al-Mg alloy with submicrometer grain size*, Acta Mater., **44**, *7*, pp. 2973-2982, 1996.
3. NAKASHIMA, K., HORITA, Z., NEMOTO, M., LANGDON, T.G., *Development of a multi-pass facility for equal-channel angular pressing to high total strains*, Mater. Sci. Eng. A., **281**, *1*, pp. 82-87, 2000.
4. PARSA, M.H., NADERI, M., NILI-AHMADABADI, M., ASADPOUR, H., *The evolution of strain during equal channel angular pressing*, Int. J. Mater. Form., **1**, *1*, pp. 93-96, 2008.
5. MEYER, L.W., HOCKAUF, M., ZILLMANN, B., SCHNEIDER, I., *Strength, ductility and impact toughness of the magnesium alloy AZ31B after equal-channel angular pressing*, Int. J. Mater. Form., **2**, *1*, pp. 61-64.
6. MORADI, M., NILI-AHMADABADI, M., HEIDARIAN, B., *Improvement of mechanical properties of Al (A356) cast alloy processed by ECAP with different heat treatments*, Int. J. Mater. Form, **2**, *1*, pp. 85-88, 2008.
7. ZHA, M., LI, Y., MATHIESEN, R.H., BJØRGE, R., ROVEN, H.J., *Microstructure evolution and mechanical behavior of a binary Al–7Mg alloy processed by equal-channel angular pressing*, Acta Materialia, **84**, pp. 42-54, 2015.
8. LU, S.K., LIU, H.Y., YU, L., JIANG, Y.L., SU, J.H., *3D FEM simulations for the homogeneity of plastic deformation in aluminum alloy HS6061-T6 during ECAP*, Procedia Eng., **12**, pp. 35-40, 2011.
9. DJAVANROODI, F., EBRAHIMI, M., *Effect of die channel angle, friction and back pressure in the equal channel angular pressing using 3D finite element simulation*, Mater. Sci. Eng. A., **527**, pp. 1230-1235, 2010.
10. BAHLOUL, R., BEN-ELECHI, S., POTIRON, A., *Optimisation of springback predicted by experimental and numerical approach by using response surface methodology*, J. Mater. Process Technol., **173**, *1*, pp. 101-110, 2006.

11. AZAOUZI, M., LEBAAL, N., *Tool path optimization for single point incremental sheet forming using response surface method*, Simul. Model. Pract. Th., **24**, pp. 49-58, 2012.
12. QIAN, L., PING, Y., YUNBAI, L., *Response surface modeling and optimization of a new impact-toughened mould material used in the shaping of sanitary ware*, Mater. Des., **50**, pp. 191-197, 2013.
13. MAKADIA, A.J., NANAVATI, J.I., *Optimisation of machining parameters for turning operations based on response surface methodology*, Measurement, **46**, *4*, pp. 1521-1529, 2013.
14. BARTZ-BEIELSTEIN, T., CHIARANDINI, M., PAQUETE, L., *Experimental methods for the analysis of optimization algorithms*, Springer, 2010.
15. KAMI, A., MOLLAEI DARIANI, B., SADOUGH VANINI, A., COMSA, D. S., BANABIC, D., *Application of a GTN damage model to predict the fracture of metallic sheets subjected to deep-drawing*, Proc. Rom. Acad. Series A, **15**, *3*, pp. 300-309, 2014.
16. * * *, *Design-Expert® software User's guide*, Trail version 7.0, Minneapolis, 2005.
17. CHANG, C.P., SUN, P.L., KAO, P.W., *Deformation induced grain boundaries in commercially pure aluminium*, Acta Mater., **48**, *13*, pp. 3377-3385, 2000.
18. VALIEV, R.Z., MULYUKOV, R.R., OVCHINNIKOV, V.V., SHABASHOV, V.A., *Mössbauer analysis of submicrometer grained iron*, Scripta Metall. Mater., **25**, *12*, pp. 2717-2722, 1991.

Received March 3, 2015